

THE 18 μm LUMINOSITY FUNCTION OF GALAXIES WITH AKARI

YOSHIKI TOBA^{1,2}, SHINKI OYABU³, HIDEO MATSUHARA², DAISUKE ISHIHARA³, MATT MALKAN⁴, TAKEHIKO WADA², YOUICHI OHYAMA⁵, HIROKAZU KATAZA², AND SATOSHI TAKITA²

¹Department of Space and Astronautical Science, the Graduate University for Advanced Studies (Sokendai), 3-1-1 Yoshinodai, Chuo-ku, Sagamihara, 252-5210 Kanagawa, Japan

²Institute of Space and Astronautical Science, Japan Aerospace Exploration Agency, 3-1-1 Yoshinodai, Chuo-ku, Sagamihara, Kanagawa, 252-5210, Japan

³Graduate School of Science, Nagoya University, Furo-cho, Chikusa-ku, Nagoya 464-8602

⁴Department of Physics and Astronomy, University of California, Los Angeles, CA 90095-1547, USA

⁵Academia Sinica, Institute of Astronomy and Astrophysics, Taiwan

E-mail: toba@ir.isas.jaxa.jp

(Received June 30, 2012; Accepted August 02, 2012)

ABSTRACT

We present the 18 μm luminosity function (LF) of galaxies at $0.006 < z < 0.8$ (the average redshift is ~ 0.04) using the AKARI mid-infrared All-Sky Survey catalogue. We have selected 243 galaxies at 18 μm from the Sloan Digital Sky Survey (SDSS) spectroscopic region. These galaxies then have been classified into five types; Seyfert 1 galaxies (Sy1, including quasars), Seyfert 2 galaxies (Sy2), low ionization narrow emission line galaxies (LINER), galaxies that are likely to contain both star formation and Active Galactic Nuclei (AGN) activities (composites), and star forming galaxies (SF) using optical emission lines such as the line width of $\text{H}\alpha$ or the emission line ratios of $[\text{OIII}]/\text{H}\beta$ and $[\text{NII}]/\text{H}\alpha$. As a result of constructing the LF of Sy1 and Sy2, we found the following results; (i) the number density ratio of Sy2 to Sy1 is 1.64 ± 0.37 , larger than the results obtained from optical LF and (ii) the fraction of Sy2 in the entire AGN population may decrease with 18 μm luminosity. These results suggest that most of the AGNs in the local universe are obscured by dust and the torus structure probably depends on the mid-infrared luminosity.

Key words: infrared: galaxy, luminosity function; conferences: proceedings

1. INTRODUCTION

The luminosity function (LF) of galaxies is one of the fundamental statistics to describe the properties of galaxies. In particular, the infrared (IR) luminosity function is an important probe of galaxy activity and the galaxy formation history hidden by dust since dust-reprocessed radiation from the Supermassive Black Hole (SMBH) or young stars is re-emitted mainly in the IR region. Until now, many LF works at mid-infrared (MIR) and far-infrared (FIR) wavelengths have been made based on the Infrared Astronomical Satellite (IRAS), the Infrared Space Observatory (ISO), the Spitzer Space Telescope, the Herschel Space

Observatory, and the AKARI satellite. These studies have advantages. LFs obtained from IRAS have treated wide sky coverage of samples. For example, Saunders et al. (1990) presented a local LF of 60 μm from 2,818 galaxies at galactic latitude $|b| > 20^\circ$ and found evidence of strong evolution. Rush et al. (1993) selected a 12 μm flux-limited sample and calculated the LFs for various types of galaxies at $|b| > 25^\circ$. But, these sample's redshift is relatively low ($z < 0.1$). On the other hand, ISO and Spitzer's samples have included more high redshift sources. For example, Pozzi et al. (2004) presented 15 μm LFs from the European Large Area ISO Survey (ELAIS) southern fields up to $z \sim 1$. Rodighiero

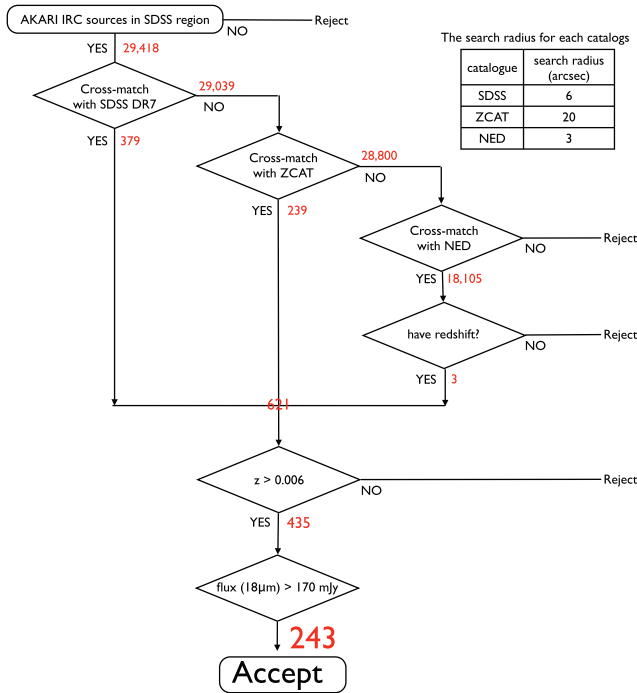


Fig. 1. The flow chart shows the process for sample selection. We adopt the search radius for the SDSS, ZCAT, and NED as 6, 20, and 3 arcsec, respectively.

et al. (2010) described mid- and far-infrared LFs from Spitzer observations of sources up to $z \sim 2.5$. More recently, Dye et al. (2010) determined the LF of 250 μm -selected galaxies with Herschel-ATLAS project out to a redshift of $z = 0.5$. But, these samples cover a relatively small area (\sim a few square degrees).

So, we focused on the AKARI All-Sky Survey to get LFs from fainter objects than IRAS and to examine wider sky coverage than ISO, Spitzer, and Herschel. The main advantage of using AKARI is that no one described the 9 μm and 18 μm LFs since only AKARI has these bands. The infrared astronomical satellite AKARI, the first Japanese space satellite dedicated to infrared astronomy, was launched on 2006. One of the most important results of AKARI is an all-sky survey in the MIR and FIR (Ishihara et al., 2010; Yamamura et al., 2010). Their spatial resolution and sensitivities are much better than those of IRAS which previously performed an all-sky survey. In particular, the detection limits (5σ) for point sources per scan are 50 and 90 mJy for the 9 and 18 μm bands, respectively, with spatial resolutions of about 5 arcsec, thus surpassing the IRAS survey in the 12 and 25 μm bands by an order of magnitude in both sensitivities and spatial resolutions.

Throughout this paper, we assume a flat Universe with $\Omega_k = 0$ and we adopt a cosmology with $(\Omega_M, \Omega_\Lambda) = (0.3, 0.7)$ and $H_0 = 75 \text{ km s}^{-1} \text{ Mpc}^{-1}$.

2. METHODS

The sample selection is performed using AKARI MIR sources together with the Sloan Digital Sky Survey (SDSS) Data Release 7 (Abazajian et al., 2009), the Center for Astrophysics (CfA) redshift survey (ZCAT: Huchra et al., 1995), and the NASA/IPAC Extragalactic Database (NED). The flow chart of the sample selection is shown in Fig. 1. First, our sample was obtained from 29,418 AKARI sources in the SDSS spectroscopic region. We identified the AKARI sources with the SDSS spectroscopic catalogue, the ZCAT, and the NED. The search radii for the SDSS, ZCAT, and NED were 6, 20, and 3 arcsec, respectively. These radii are determined considering the position accuracy and the full-width-half-maximum (FWHM) of the point spread function (PSF) for AKARI MIR sources. Then, we excluded 186 nearby galaxies with $z < 0.006$ from the sample because of the following reason. An error in distance measurement is dominated by a peculiar motion for the galaxies with $z < 0.006$, and thus, the luminosity also has a large error. Furthermore, to ensure the flux accuracy, we extracted objects with flux at 18 $\mu\text{m} > 170 \text{ mJy}$. This flux corresponds to 50% completeness flux limit calculated by Kataza et al. (2010). As a result, 243 galaxies were selected for constructing the 18 μm LFs.

We then classified these 243 galaxies into five types: Seyfert 1 galaxies (Sy1), Seyfert 2 galaxies (Sy2), low ionization narrow emission line galaxies (LINER), galaxies that are likely to contain both star formation and AGN activity (composite types of galaxies, hereafter Composite), and star forming galaxies (SF) using the optical line flux. First, we separated Sy1 (including quasars) using the FWHM of the $\text{H}\alpha$ emission line. We extracted objects with FWHM ($\text{H}\alpha$) greater than 1,200 km s^{-1} as Sy1 in the same way as Hao et al. (2005a). For the objects that have an $\text{H}\alpha$ emission line with FWHM $< 1,200 \text{ km s}^{-1}$, we classified the galaxies into Sy2, LINER, Composite, and SF by using the optical flux line ratios such as $[\text{OIII}]\lambda 5007/\text{H}\beta$ versus $[\text{NII}]\lambda 6583/\text{H}\alpha$ (Baldwin et al., 1981). For the objects that do not have the information of these line fluxes, we classified them according to previous literatures.

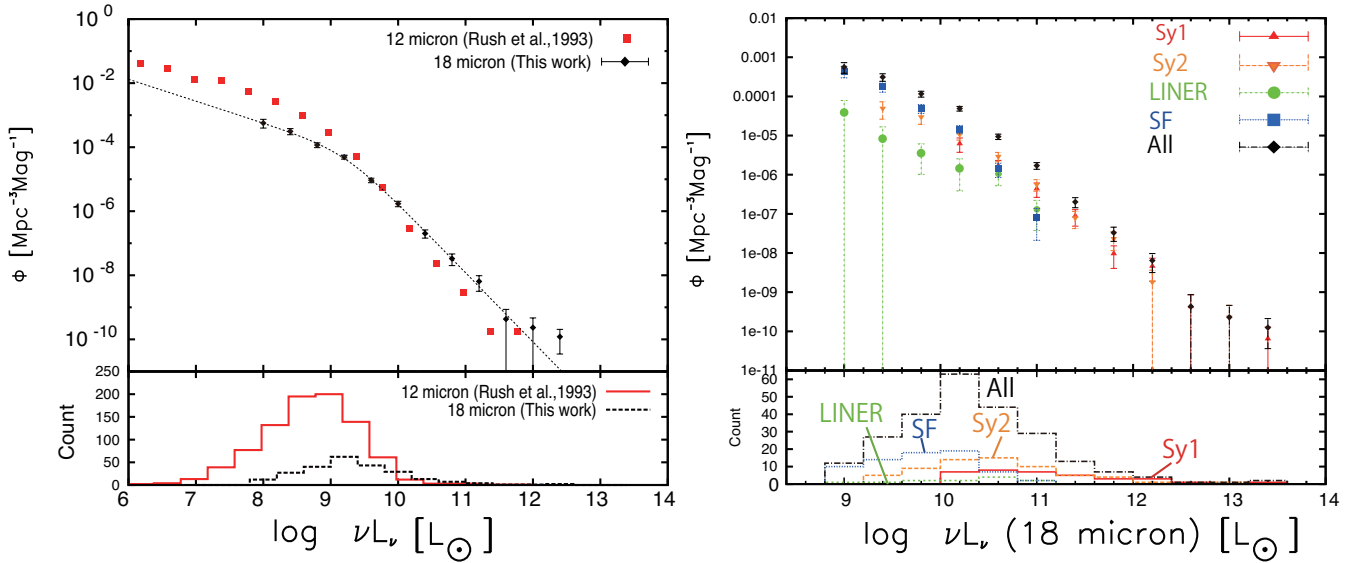


Fig. 2. The 18 μm LFs for all galaxies (left) and each types of galaxies (right), plotted in terms of volume density as a function of luminosity. The 12 μm LFs (Rush et al., 1993) is also plotted for comparison. The error bar represents the Poisson-statistical uncertainty.

3. RESULTS

Here we obtain the LFs (i.e. the volume density of galaxies per unit magnitude range) of our AKARI MIR galaxies. The LFs are derived by following the $1/V_{\text{max}}$ method as described by Schmidt (1968). The volume density $\phi(L)$ and its uncertainty $\sigma_{\phi(L)}$ were derived using the expressions

$$\phi(L) = \sum_i^N \frac{1}{V_{\text{max},i}}, \quad (1)$$

$$\sigma_{\phi(L)} = \sqrt{\sum_i^N \frac{1}{V_{\text{max},i}^2}}, \quad (2)$$

where V_{max} is the maximum co-moving volume of i th galaxies after applying K-correction and completeness correction, and the sum is over all galaxies in each luminosity bin.

The LF for Sy1, Sy2, LINER, SF, and all galaxies at 18 μm is given in Fig. 2. The shape of LFs obtained from previous work (Rush et al., 1993) are in good agreement with our determinations within the error, except the low-luminosity region. The cause of the differences in the low-luminosity regime is possibly the effect of local inhomogeneities (particularly the Virgo supercluster) in the IRAS survey, as suggested by many authors (e.g. Fang et al., 1998).

4. DISCUSSION

4.1. The Number Density Ratio of Sy1 and Sy2

We compare the number density of Sy1 with that of Sy2 in order to restrict the structure of the dust torus. For this purpose, we assume that the MIR luminosity of Sy1 and Sy2 should be the same if they have the same scale of the central engine. This assumption predicts that the ratio of the infrared luminosity from the dust torus to the X-ray luminosity from the central engine L_{MIR}/L_X to be independent of Seyfert type, which is confirmed by some authors (e.g. Lutz et al., 2004).

By integrating the LFs of Sy1 and Sy2 separately, we obtained the number density ratio, $\Phi_{\text{Sy2}}/\Phi_{\text{Sy1}}$, which is given by the following formula,

$$\Phi = \int_L \phi(L) dL \sim \sum_i \phi(i) \Delta L. \quad (3)$$

In this work, the integral range is $\log(\nu L_\nu) > 10^{10} L_\odot$ for both Sys. Our results of the number density ratio of Sy2 to Sy1, $\Phi_{\text{Sy2}}/\Phi_{\text{Sy1}}$, is 1.64 ± 0.37 . We then compared this value with some previous results obtained from the optical LFs (Hao et al., 2005b), IR LFs (Rush et al., 1993), and hard X-ray LFs (Burlon et al., 2011). Note that before comparing these results with our result, we converted each νL_ν into $\nu L_{18\mu\text{m}}$ using SED templates (Shang et al., 2011).

The results obtained from the [OIII] LF in Hao et

al. (2005b) is 1.10 ± 0.07 , smaller than that of our work. This difference is probably due to that the [OIII] photons are absorbed by the dust torus, especially for Sy2. The results obtained from $12 \mu\text{m}$ and the hard X-ray LF are 1.75 and 1.63, respectively, which are in good agreement with our works. These results indicate that there is a large number of dusty AGNs in the local universe. The result mentioned above is consistent with previous works with X-ray observation (e.g. Malizia et al., 2009).

4.2. Implication for the Covering Factor of Dust Torus

As shown in the right panel of Fig. 2, the number density ratio of Sy2 to Sy1 changes with $18 \mu\text{m}$ luminosity. In other words, the fraction of Sy2 in the entire AGN population seems to decrease with higher $18 \mu\text{m}$ luminosity. This tendency probably means that the luminosity from the central engine has influenced the structure of the torus; the opening angle of the dust torus is larger for more luminous AGNs, probably because increasing the luminosity means more sublimated dust, and thus the broad-line emission can be seen through a larger opening angle as reported by Lawrence (1991). This result has been reported several times in previous works such as Burlon et al. (2011). Therefore, we were able to confirm this tendency from the viewpoint of IR using AKARI.

REFERENCES

- Abazajian, K. N., et al., 2009, The Seventh Data Release of the Sloan Digital Sky Survey, *ApJS*, 182, 543
- Baldwin, J. A., Phillips, M. M., & Terlevich, R., 1981, Classification Parameters for the Emission-Line Spectra of Extragalactic Objects, *PASP*, 93, 5
- Burlon, D., et al., 2011, Three-year Swift-BAT Survey of Active Galactic Nuclei: Reconciling Theory and Observations?, *AJ*, 728, 58
- Dye, S., et al., 2010, Herschel-ATLAS: Evolution of the $250 \mu\text{m}$ Luminosity Function out to $z = 0.5$, *A&A*, 518, L10
- Fang, F., Shupe, D. L., Xu, C., & Hacking, P. B., 1998, The Mid-Infrared Color-Luminosity Relation and the Local 12 Micron Luminosity Function, *AJ*, 500, 693
- Hao, L., et al., 2005, Active Galactic Nuclei in the Sloan Digital Sky Survey. II. Emission-Line Luminosity Function, *AJ*, 129, 1795
- Hao, L., et al., 2005, Active Galactic Nuclei in the Sloan Digital Sky Survey. I. Sample Selection, *AJ*, 129, 1783
- Huchra, J. P., Geller, M. J., & Corwin, H. G., Jr., 1995, The CfA Redshift Survey: Data for the NGP +36 Zone, *ApJS*, 99, 391
- Ishihara, D., et al., 2010, The AKARI/IRC Mid-Infrared All-Sky Survey, *A&A*, 514, 1
- Kataza, H., et al., 2010, AKARI/IRC Point Source Catalogue Version 1.0 -Release Note (Rev.1)
- Lutz, D., Maiolino, R., Spoon, H. W. W., & Moorwood, A. F. M., 2004, The Relation between AGN Hard X-Ray Emission and Mid-Infrared Continuum from ISO Spectra: Scatter and Unification Aspects, *A&A*, 418, 465
- Lawrence, A., 1991, The Relative Frequency of Broad-Lined and Narrow-Lined Active Galactic Nuclei - Implications for Unified Schemes, *MNRAS*, 252, 586
- Malizia, A., et al., 2009, The Fraction of Compton-Thick Sources in an INTEGRAL Complete AGN Sample, *MNRAS*, 399, 944
- Pozzi, F., et al., 2004, The Mid-Infrared Luminosity Function of Galaxies in the European Large Area Infrared Space Observatory Survey Southern Fields, *AJ*, 609, 122
- Rodighiero, G., et al., 2010, Mid- and Far-Infrared Luminosity Functions and Galaxy Evolution from Multiwavelength Spitzer Observations up to $z = 2.5$, *A&A*, 515, 8
- Rush, B., Malkan, M. A., & Spinoglio, L., 1993, The Extended 12 Micron Galaxy Sample, *ApJS*, 89, 1
- Saunders, W., et al., 1990, The 60-Micron and Far-Infrared Luminosity Functions of IRAS Galaxies, *MNRAS*, 242, 318
- Schmidt, M., 1968, Space Distribution and Luminosity Functions of Quasi-Stellar Radio Sources, *AJ*, 151, 393
- Shang, Z., et al., 2011, The Next Generation Atlas of Quasar Spectral Energy Distributions from Radio to X-Rays, *ApJS* 196, 2
- Yamamura, I., et al., 2010, AKARI/FIS All-Sky Survey Point Source Catalogues (ISAS/JAXA, 2010), *yCat*, 2298, 0